CHAPTER 4

4.1 Introduction

Synthetic chemistry requires powerful tools for building at will complex chemical structures in a modular fashion from simple blocks.[1] This goal has been partially achieved at the molecular level through formation of covalent bonds by templated self-assembly.[2] However, despite the fact that here are also some interesting examples of large self-assembled structures,[3] standardized procedures for the step-by-step synthesis of nanoscopic structures are still not well known and codified.[4] A better understanding of such processes, however, would facilitate the design of molecular building blocks for the construction of complex functional architectures and "smart" materials for applications in molecular electronics and mechanics. Functionalized surfaces could in principle be used as shape persistent supports for the reversible assembly of two-dimensional architectures. If layer-by-layer techniques were used, even the construction of three-dimensional nanoscale objects should be feasible. A key factor in such directed nanochemistry is the availability of a suitable casting mould or, in other words, the placing of preferably

1. a) C. J. Hawker, K. L. Wooley, *Science* **2005**, *309*, 1200; b) U. Hahn, M. Elhabiri, A. Trabolsi, H. Herschbach, E. Leize, A. van Dorsselaer, A.-M. Albrecht-Gary, J.-F. Nierengarten, *Angew. Chem. Int. Ed.* **2005**, *44*, 5338 (c) H. C. Kolb, M. G. Finn, K. B. Sharpless, *Angew. Chem. Int. Ed.* **2001**, *40*, 2004.
2. R. Vilar, *Struct. Bonding* **2004**, *111*, 85.
3. D. N. Reinhoudt, M. Crego-Calama, *Science* **2002**, *295*, 2403
4. Only recently, Ercolani raised new doubts that cooperative effects are one of the main driving forces in classical supramolecular self-assembled structures, see G. Ercolani, *J. Am. Chem. Soc.* **2003**, *125,* 16097.

noncovalent binding or "trapping" sites such as calixarenes or cyclodextrins in a predefined manner on the surface of a support. The function of these trapping sites is to assemble either a number of single guests, for example, for further layer-by-layer growth or the assembly of network aggregates, or to allow larger objects with several binding sites to dock to the surface at various sites (see Figure 4.1).[5] The latter approach is much like placing an EPROM at its designated position on a circuit board of an electronic device. Especially attractive are those examples where the assembly/disassembly processes are coupled with

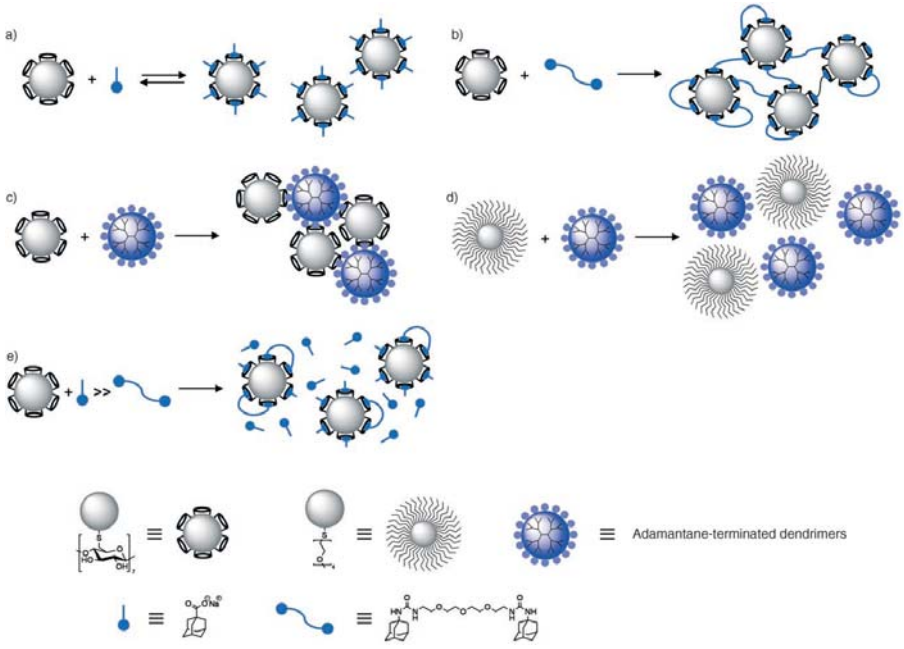

Figure 4.1. Different aggregation protocols of CD-functionalized AuNPs with adamantyl-containing guest molecules.

5. a) Crespo-Biel, A. Jukovic, M. Karlsson, D. N. Reinhoudt, J. Huskens, *Isr. J. Chem.* **2005**, *45*, 353 b) A. Mulder, J. Huskens, D. N. Reinhoudt, *Org. Biomol. Chem.* **2004**, *2*, 3409

switching protocols that allow reversible control over the building process. In a previous work of our research group calix[4]arene derivatives have been functionalized with alkanethiol chains of two different lengths (six or eleven carbon atoms), and two sets of nanoparticles with different amounts of appended calixarene were prepared (see Figure 4.2).[6]

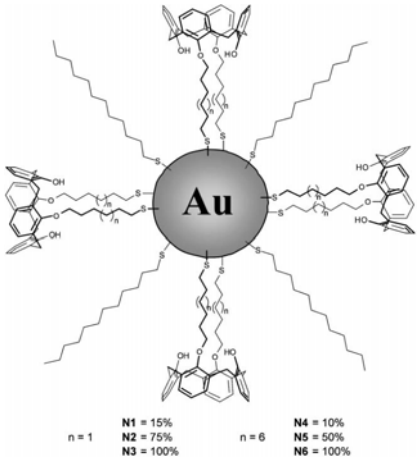

Figure 4.2. Au MMPCs stabilized by calix[4]arene derivatives.

The choice to append 1,3-dialkoxycalixarene derivatives onto the gold surface was dictated by their well known recognition properties toward quaternary ammonium cations.[7] We found from ^{1}H NMR titrations in $CDCl_3$ that the hosts supported onto the clusters experience stronger binding in solution than the free calixarenes. Moreover, the efficiency of binding was positively affected by the number of calixarene units present on the gold core.[6] Interestingly, an increase in the length of

6. A. Arduini, D. Demuru, A. Pochini, A. Secchi, *Chem. Commun.* **2005**, 645
7. a) A. Arduini, A. Secchi, A. Pochini, *Eur. J. Org.* **2000**, 2325; b) A. Arduini, G. Giorgi, A. Pochini, A. Secchi, F. Ugozzoli, *J. Org. Chem.* **2001**, *66*, 8302; c) A. Arduini, E. Brindani, G. Giorgi, A. Pochini, A. Secchi, *J. Org. Chem.* **2002**, *67*, 6188.

the spacer between the particle surface and the calix[4]arene also led to dramatically enhanced recognition in a solvent of medium polarity such as chloroform. This is an interesting case of radial coordination amplification that appears to be an exclusive feature of clusters and nanoparticles.

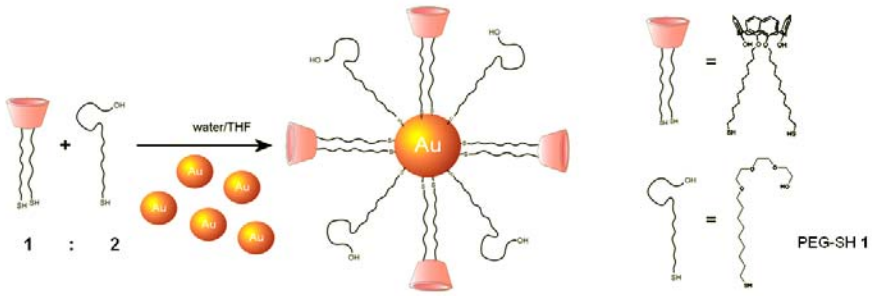

Figure 4.3. Water soluble Au MMPCs stabilized by calix[4]arene derivatives.

In another paper it has been demonstrate that these systems work also in aqueous media.[8] The molecular recognition properties in water of the particle-bound calixarene, prepared as depicted in figure 4.3, are qualitatively demonstrated by specific binding studies using two different chemically modified substrates (see Figure 4.4).

In the simplest case, the nanoparticles bind specifically from aqueous solution to the molecular sieve beads primed with pyridinium ions indicating that the cavity of the calix[4]arene presents onto the gold surface exhibits its characteristic cation binding properties also in aqueous media and when immobilized in the ligand shell of the MPCs. This binding interaction is easily observed with the naked eye owing to the intense red color of the gold nanoparticles (see Figure 4.4b). A

8. T. R. Tshikhudo, D. Demuru, Z. Wang, M. Brust, A. Secchi, A. Arduini, A. Pochini, *Angew. Chem. Int. Ed.* **2005**, *44*, 2913.

number of control experiments clearly confirmed that both the pyridinium and the calixarene moieties have to be present to achieve any attachment of MPCs to the molecular sieve beads.

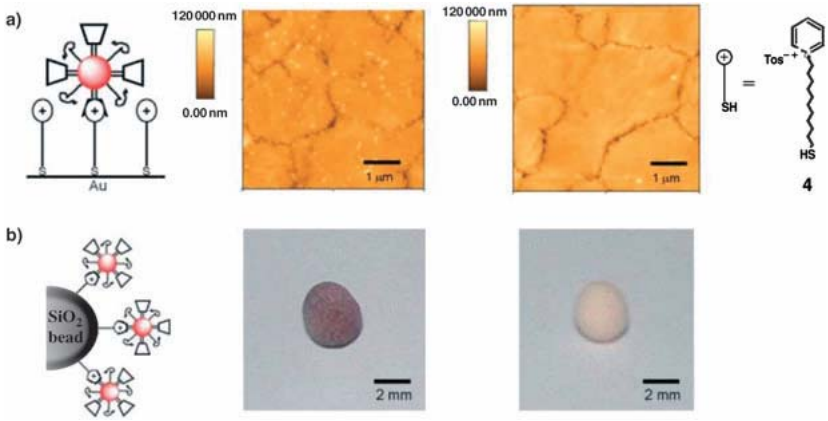

Figure 4.4. Specific binding in water of calixarene-modified gold nanoparticles with alkylated pyridinium ions inserted onto different substrates: a) gold surface and b) silica beads (see text for further experimental details).

Further binding studies were carried out by AFM using a self-assembled monolayer (SAM) of pyridinium ions on a flat gold surface as the substrate. As demonstrated from the AFM images depicted in Figure 4.4a, the calixarene modified nanoparticles bind selectively to this SAM from aqueous solution, while binding to clean gold surfaces occurred only as a non-specific minority event. MPCs without calixarene in their ligand shell did not show any significant binding to the SAMs or to clean gold surfaces.

4.2 Self-assembly of gold nanoparticles in solution

In the previous paragraph it has been shown that preorganized calix[4]arene derivatives supported onto gold clusters can act as recognition binding sites for organic cations both in acqueos and organic media. The aim of the following discussion is to present our studies aimed to exploit the calix[4]arene cavity of the receptor **1** (see Formula) to self-assemble gold clusters through weak supramolecular interactions.[9]

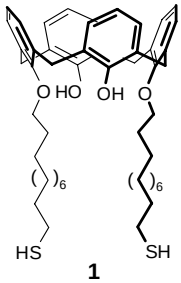

1

The idea to self-assemble gold nanoparticles is not new. Indeed, in the literature are present several examples that show the feasibility of these processes either in solutions[10,5a] or onto surface using cyclodextrins.[11] However, the possibility to exploit the calixarene cavity in this context is certainly quite unexplored.

The study of this type of phenomenon would require that a) clusters association afford variation in observable physical properties and b) the

9. The work presented in this chapter has been carried out at CAP (Center for Applied Photonics) of the University of Konstanz (Germany) in the research group of Dr. Anton Plech from April 2007 to July 2007.
10. a) S.-Y. Lin, S.-W. Liu, C.-M. Lin, C. Chen *Anal. Chem.* **2002**, *74*, 330; b) S. O. Obare, R. E. Hollowell, C. J. Murphy, *Langmuir* **2002**, *18,* 10407
11. O. Crespo-Biel, B. Dordi, D. N. Reinhoudt, J. Huskens, *J. Am. Chem. Soc.* **2005**, *127*, 7594.

design of suitable bifunctional guests. As bifunctional guests we define an organic compound characterized by two domains (identical or not) specifically able to associate simultaneously, through reversible supramolecular interactions, with two host molecules localized on different nanoparticles.

In order to satisfy requisite a) we decided to synthesize new Au MPCs stabilized by **1** characterized by a significant SPB (surface plasmon band). In this way the self-assembly process can be studies using optical techniques. The clusters synthesis was carried out through ligand-place exchange reactions between tetraoctylammonium bromide-stabilized Au MPCS[12] having a core diameter of 5–8 nm and the bidentate calix[4]arene **1** (see Figure 4.5). This exchange reaction takes place because the S-Au bond is more stable than the electrostatic interaction between Au and Br^-. The resulting calix[4]arene MPCs (C4NPs) showed a good solubility in most organic solvents like toluene, chloroform and dichloromethane.

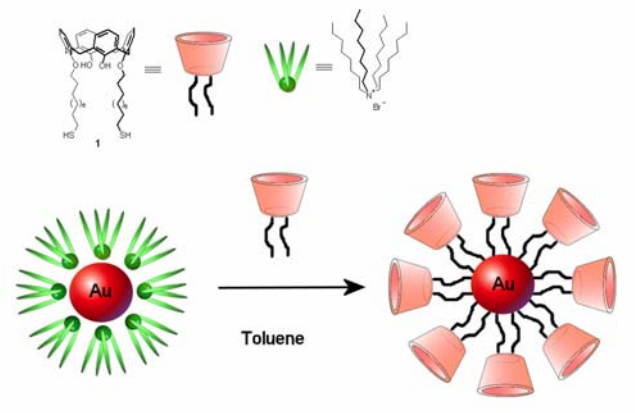

Figure 4.5. Synthesis of C4NPs trough ligand-place exchange reactions.

12. J. Fink, C. J. Kiely, D. Bethell, D. J. Schiffrin *Chem. Mater.* **1998,** *10,* 922

The C4NP clusters were characterized by UV-vis spectroscopy and TEM analysis. The exchange reaction did not substantially changed the distribution size of the metallic core. Indeed, the UV spectrum in chloroform depicted in figure 4.6 evidenced only a small red shift of the main absorption band. TEM images then confirmed that the calix[4]arene-coated clusters are characterized by a mean core diameter of ≈ 7 nm (see Figure 4.7).

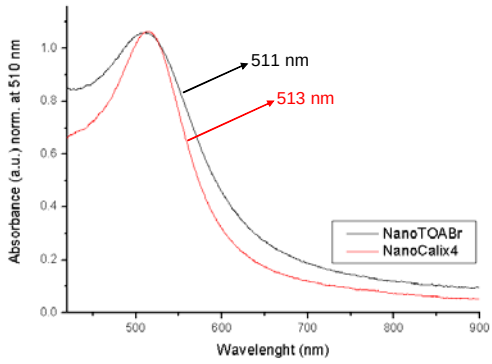

Figure 4.6. UV-Vis spectra of TOABr-stabilized (red line) and C4NP (black line) Au MPCs in chloroform.

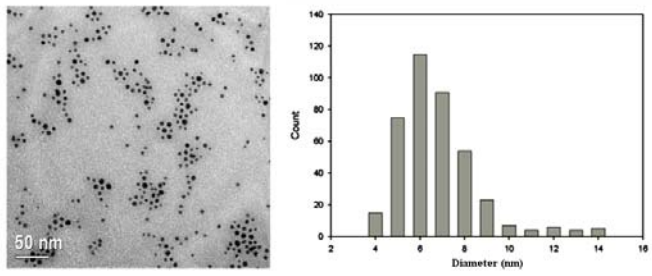

Figure 4.7. TEM image and core size distribution diagram of the C4NP Au MPCs.

The first guest used for the self-assembly process was the rigid dimethylviologen ditosilate (DMV×2Ts, see Figure 4.8).

The drop-wise addition of a 10^{-5} M solution of DMV×2Ts in chloroform to a solution of C4NP in chloroform initially determines a blu-shift of the main absorption band of the clusters (see Figure 4.8).

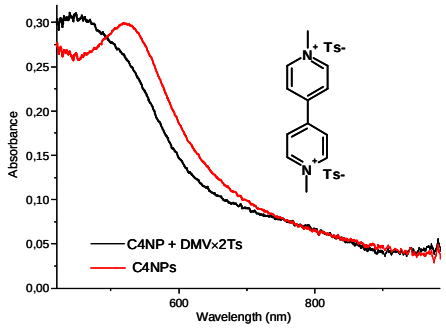

Figure 4.8. UV-Vis spectra of the solution of C4NP Au MPCs before (red line) and after the addition of a 10^{-5} M of DMV×2Ts in chloroform.

Unfortunately, the further addition of the dicationic salt solution causes the precipitation of a black solid material from the solution. This phenomenon it is probably to ascribe to the rigid structure of the dimethyl viologen salt that creates a large 3D-network of self-assembled nanoparticles (see Figure 4.9).

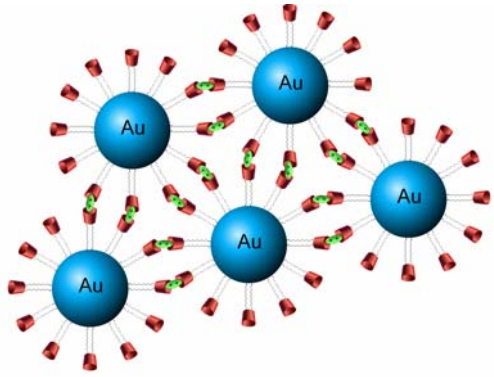

Figure 4.9. Schematic representation of the hypothesized 3D network of self-assembled Au MPCs (C4NP) induced by the complexation with DMV×2Ts.

The solid filtered-off from the solution was insoluble even in very polar solvents such as DMF and DMSO. Considering a very simplified binding model, it is possible to assume that the aggregation process between clusters follows the pathways described in figure 4.10. In particular in the first stage of the guest addition, when it is presumed that the difunctional guest G-G is in large defect with respect the recognition sites present onto the clusters surfaces, a first equilibrium governed by a $K_{1:1}$ will occur with the formation of the supra-adduct MPC ⊃G-G (see Figure 4.10a).

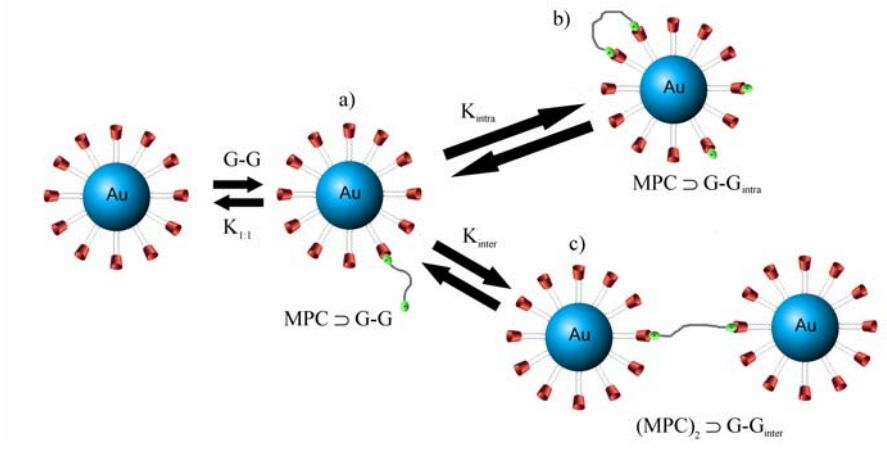

Figure 4.10. Simplified binding model between Au MPCs and bifunctional guests.

Such an adduct can thus evolve, through two different competitive equilibrium, in an intramolecular supra-adduct MPC ⊃G-$G_{(intra)}$ where two adjacent recognition sites are complexed by the difunctional guest (see Figure 4.10b); or an intermolecular supra-aggregate $(MPC)_2$⊃G-$G_{(inter)}$ (see Figure 4.10c). The two competitive equilibria are governed by a K_{intra} and a K_{inter}, respectively. Both are enthalpically driven, but the latter is certainly entropically unfavoured, therefore it is reasonable to

assume that for this model $K_{intra} > K_{inter}$. However, the fate of MPC ⊃G-G will be strongly affected by the nature (length and flexibility) of the difunctional guest. Indeed, the very rigid DMV×2Ts induces exclusively the formation of intermolecular supra-aggregates.

To overcome this problem, 1,1'-(pentane-1,5-diyl)dipyridinium diiodide (Space5×2I) and 1,1'-(decane-1,10-diyl)dipyridinium diiodide (Space10×2I) have been used as flexible difunctional guests (see formula).[13]

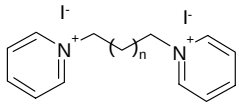

n = 3 **space 5 x 2I**
n = 8 **space 10 x 2I**

The structure of Space5 dication should be mobile enough to prevent the strong aggregation observed with DMV. Moreover, considering the geometry of the complexes formed between the calix[4]arene cavity and alkyl pyridinium cation, the length of the alkyl chain separating the two pyridinium moieties should strongly disfavour the formation of intra-molecular complexes.[14]

A new experiment was thus devised: to a stirred solution of C4NPs in chloroform a solution 10^{-4} M of Space5×2I was drop-wise added. The results of the titration experiments have been depicted in Figure 4.11.[15]

---

13. F. Zheng, E. Bayram, S. P. Sumithran,J. T. Ayers, C.-G. Zhan, J. D. Schmitt, L. P. Dwoskin, P. A. Crooks, *Bioorg. Med. Chem.* **2006**, *14*, 3017.
14. A. Arduini, A. Secchi, A.Pochini, *Eur. J. Org.* **2000**, 2325.
15. It should be observed that an estimate of the average number of recognition sites present onto the surface of the clusters is still under progress. Therefore, the evaluation of the clusters aggregation induced by the guest should be exclusively considered as semiqualitative.

Absorption spectroscopy mainly detects the plasmon resonance band of the clusters. The maximum of this band is sensitive to the size of the particles as well as to particle-particle electromagnetic coupling. Before guest addition, the UV spectrum shows a resonance corresponding to the uncomplexed particles at $\lambda = 510$ nm. Upon guest addition a second new and broad plasmon resonance band starts to appear at higher wavelength ($\lambda \approx 600$ nm) appears. It is possible to notice in the inset of figure 4.11, however, that for very low concentrations of the guest ($0.1\text{-}1\times10^{-6}$M) the 510 and 600 nm extinctions not change appreciably.

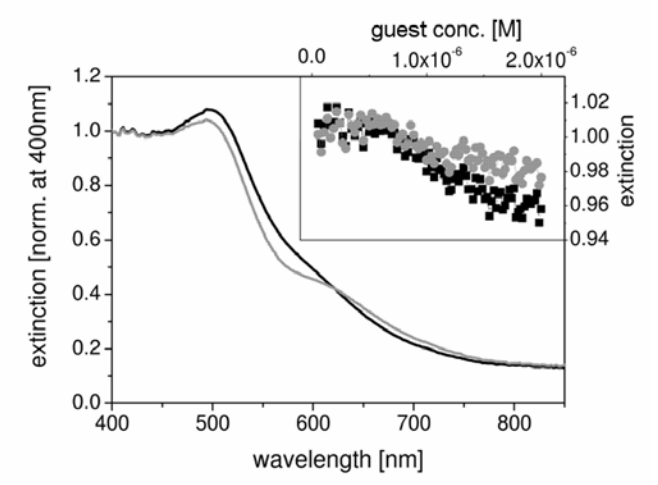

Figure 4.11. UV-Vis spectroscopic titration of C4NPs Au MPCs with Space5×2I in chloroform solution. For clarity only the spectra of the "uncomplexed" clusters (black line) and of the resulting "aggregates" (grey line) obtained at end of the titration are presented. The variation of the extinction at $\lambda = 510$ (black squares) and 600 nm (grey circles) upon guest addition throughout all the titration has been summarized in the inset (see text for further details).

In other words, when the guest is presumably present in solution in defect with respect the clusters there is no observable aggregation. When the concentration of the guest in solution reaches $\approx1\times10^{-6}$ M a change occurs in the UV-Vis spectra. In particular, an increasing of the

extinction at λ = 600 nm is observed, whereas the extinction at 510 nm decreases. It is known that the SPB resonance is delocalized over several particles and its position and strength depends on the particle distance and the number of particles that compose the aggregates.[16] In other words this means that during the titration an initial defined soluble supra-structure is formed that then evolves in a larger aggregate.

Dynamic Light Scattering (DLS) experiments were thus carried out in order to better rationalize this time-dependent behaviour.[17] DLS represents indeed a powerful technique for the determination of the size distribution profile of small particles in solution. When light hits small particles the light scatters in all directions (Rayleigh scattering) so long as the particles are small compared to the wavelength (<250 nm). If the light source is a laser, and thus is monochromatic and coherent, then one observes a time-dependent fluctuation in the scattering intensity. These fluctuations are due to the fact that the small molecules in solutions are undergoing Brownian motion and so the distance between the scatterers in the solution is constantly changing with time. This scattered light then undergoes either constructive or destructive interference by the surrounding particles and within this intensity fluctuation information is contained about the time scale of movement of the scatterers.

The dynamic information of the particles is then derived from an autocorrelation of the intensity trace recorded during the experiment. At short time delays the correlation is high because the particles do not have

16. a) U. Kreibig, M. Vollmer: *Optical Properties of Metal Clusters*, Springer, Berlin **1995** b) P. K. Jain, W. Huang, M. A. El-Sayed, *Nano Letters* **2007**, *7*, 2080; c) J. Schmitt, P. Mächtle, D. Eck, H. Möhwald, C. A. Helm *Langmuir* **1999**, *15,* 3256.
17. B. Chu, *Laser Light scattering: Basic Principles and Practice*, 2nd Ed., Dover Publications, ISBN: 0-486-45798-2, **2007**.

a chance to move to a great extent from the initial state that they were in. The two signals are thus essentially unchanged when compared after only a very short time interval. As the time delays become longer, the correlation starts to exponentially fall off to zero, meaning that there is no correlation between the intensity of scattering of the initial state with the final state after a long time period has elapsed (relative to the motion of the particles). This exponential decay is obviously then related to the motion of the particles specifically, the diffusion coefficient. The function used to calculate this correlation is the *autocorrelation function* that describes how a given measurement relates to itself in a time dependent manner:

$$r_\tau = \frac{\sum_{i=1}^{N-k}(Y_i - \overline{Y})(Y_{i+k} - \overline{Y})}{\sum_{i=1}^{N}(Y_i - \overline{Y})^2}$$

The decay of the autocorrelation is described by an exponential decay function $G(\tau)$ which relates the autocorrelation to the diffusion coefficient D and the measurement vector K:

$$G(\tau) \propto e^{-2DK^2\tau}$$

$$K = \frac{4\pi\eta}{\lambda}\sin\left(\frac{\theta}{2}\right)$$

where η is the refractive index of the solution λ is the wavelength of the laser (632.8 nm) and θ is the angle of scattering measurement (possible choices are: 15.2, 21.1, 31.1, 41.9, 51.8, 90 degrees). By fitting the points of autocorrelation to the function *G(t)*, the diffusion coefficient can be

measured and related to the equivalent sphere of diameter d using the Stokes-Einstein equation:

$$D = \frac{k_B T}{3\pi\eta d}$$

where η is the solvent viscosity, T is the temperature in K, D is the diffusion coefficient in m^2/s, k_B is the Boltzmann constant (1.3807×10^{-23} J/K) and d is the diameter of the sphere in m.

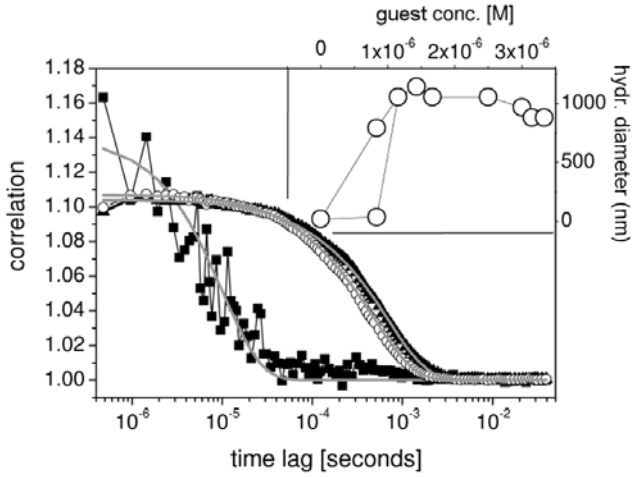

Figure 4.12 DLS titration of C4NPs Au MPCs with Space5×2I in chloroform. The black squares, white circles and black triangles represent the observed correlation function derived from light scattering for increasing amount of guest added (the lines represent their fitting with the model). The inset shows the dependence of the calculated hydrodynamic diameter of the clusters on guest addition.

The DLS experiments were performed adding increasing amounts of a chloroform solution $5x10^{-6}$ M of Space5×2I to a chloroform solution containing the C4NP Au MPCs. In Figure 4.12 have been depicted the correlation functions and their fitting for increasing guest additions. For low concentration of Space5 ($\approx 10^{-6}$ M), the light scattering of the clusters is poor and thus also the correlation function (see black squares).

Despite this the calculated hydrodynamic diameter of the clusters remains in the range of 10-20 nm (see inset).[18] Considering that organic shell around the gold core should contribute for a thickness of ≈ 2 nm (the length of calix[4]arene **1**), this diameter range is somewhat in agreement with diameter of the core determined through TEM measurement (see Figure 4.7).

When the concentration of the guest reaches $0.7\text{-}0.8\times10^{-6}$ M, the clusters start to aggregate in solution yielding good correlation curves and, as a consequence, also the value of the calculated hydrodynamic diameter (≈ 1'000 nm) undergoes an abrupt change. It should also be noticed that at this guest concentration both the isolated clusters and the aggregates are co-existent in solution (see inset). For higher guest concentration the isolated clusters disappear completely.

As in the case seen with DMV×2Ts, also these aggregates tend to collapse from the solution when a large amount of Space5 is added. However, differently from DMV×2Ts, these aggregates can be dissolved again in polar solvent such as methanol. In other words, the treatment with methanol destroy, as expected, the aggregates through the solvation of the difunctional guest. Indeed, the recovered C4NP clusters show again their typical UV spectrum.

The aggregation experiments on C4NP Au MPcs were finally repeated using the flexible Space10×2I as guest (see Figure 4.13). The UV-Vis data show that the addition of the guest determines the formation of a broad SPB at λ = 600 nm. Therefore, as found for Space5, Space10 is

[18]. An exact determination of the diameter is difficult for this range of sizes because small particles yield poor light scattering. DLS could also be biased by the biggest particles in the solution, if the suspension is heterogeneous.

able to drive the aggregation of the C4NP clusters. In this case, however, the increase of the extinction at λ = 600 nm becomes appreciable when the concentration of the guest in solution reaches $\approx 0.5\text{-}0.6\times10^{-6}$ M (see inset). In the range $0.5\text{-}1\times10^{-6}$ M the extinction at 600 nm changes smoothly. This was an indirect indication that the formation of aggregates did not occur suddenly as seen with Space5.

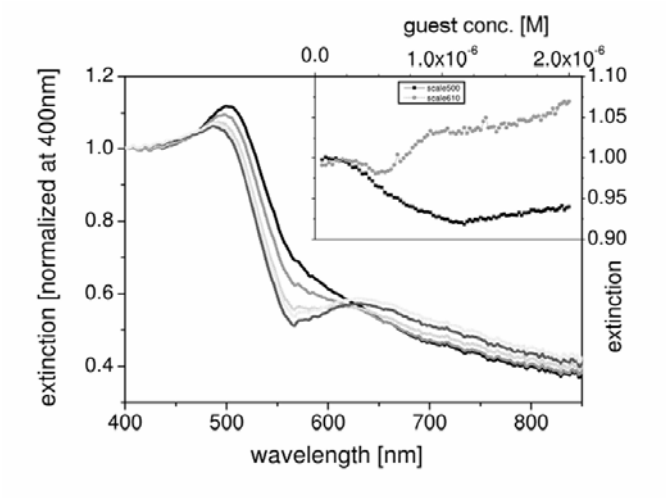

Figure 4.13. Spectroscopic titration of C4NPs Au MPCs with Space10×2I in chloroform solution. The variation of the extinction at λ = 510 (black squares) and 600 nm (grey circles) upon guest addition throughout all the titration has been summarized in the inset (see text for further details).

The dynamic of the aggregation process was then studied through DLS measurements. Good correlation functions were obtained for several addition of Space10 (see Figure 4.14), though also in this case when the guest is in large defect (up to $\approx 0.5\times10^{-6}$ M), small clusters are present in solution and the light scattering is poor (see black squares in figure 4.14). The analysis of trend of the clusters hydrodynamic diameter with the guest concentration (see inset) revealed that in the 0.5 to 1.5×10^{-6} M

concentration range there are several co-existent species present in solution: small clusters and aggregates with $d \approx$ 400-500 nm, Only when the guest concentration reaches 1.9×10^{-6} M the hydrodynamic diameter remains around 600 nm. Differently from what observed with Space5, with the more flexible Space10 the variation of the d assumes a stepwise course as the concentration of the guest in solution is increased (see Inset).

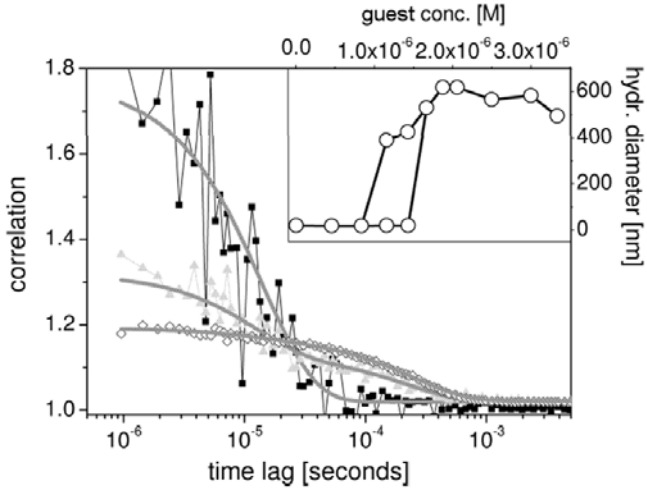

Figure 4.14. DLS titration of C4NPs Au MPCs with Space10×2I in chloroform. The inset shows the dependence of the calculated hydrodynamic diameter of the clusters on guest addition.

A possible explanation for this particular behaviour might be that when in solution the difunctional guest is present in defect with respect the clusters, the calix[4]rene units present onto the cluster surface are fully saturated, with the positively charged pyridinium "heads" through the formation of intramolecular complexes. Using our simplified model, it thus seems that in this conditions K_{intra} is higher than K_{inter}. Only when

the guest is added in excess with respect the clusters aggregation between the clusters can occur through the formation of intermolecular complexes (see Figure 4.15), where the process governed by K_{inter} is more favoured than that governed by K_{intra}. The stepwise dependence of the aggregation on guest concentration can be also explained on the basis that such process is diffusion limited, that is while a single guest diffuses quickly

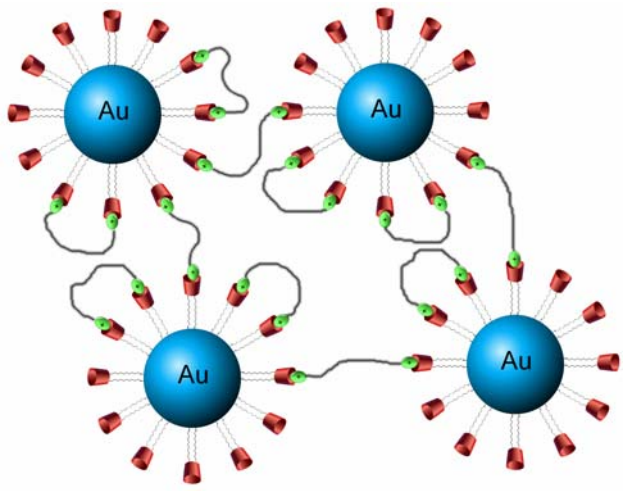

Figure 4.15. Schematic representation of interaction between C4NPs and Space10

to complex the particles, the particles diffuse slowly to find another partner for the intermolecular complexation.

To support our findings is the observation that the formed aggregates do not collapse from the chloroform solution even when a large excess of Space10×2I is added to the solution. The particular structure of Space10 dication might indeed allows the formation of intramolecular and intermolecular complexes as illustrated in figure 4.15. The noteworthy solubility experienced by this self-assembled supra-aggregate could be

explained on the base of the minor number of intermolecular links present between MPCs. Indeed, the analysis of the calculated hydrodynamic diameters shows that the aggregates formed with Space10 (500-600 nm) are smaller that those formed by Space5 (1'000 nm). It should be also considered that the linkers present in the former supra-aggregate are longer and more flexible than those found in the aggregates derived by Space5 or worse DMV. This results in a less packed aggregation that would favour the access of the solvent molecules within the 3D network of clusters.

The guest-induced aggregation of the C4NP clusters with Space10×2I was also studied through TEM measurements. From the TEM image depicted in Figure 4.16 it is possible to notice that aggregation effectively occurred. The Au MPCs are all close to each other forming a 3D packed system (see Figure 4.16a).

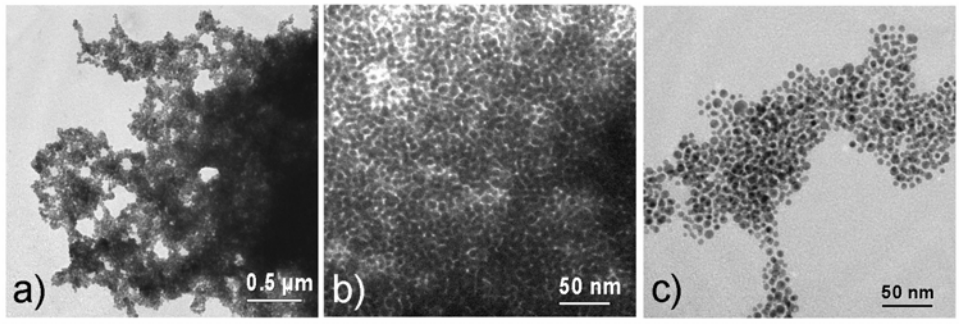

Figure 4.16. TEM images of self-assembled C4NPs with Space10

In fact, in some regions it is possible to notice where the aggregates changes from a 2D monolayer of clusters (see Figure 4.16c) to a 3D network (see Figure 4.16b) on the TEM grid.

Experimental Section

General Remarks:

All reactions were carried out under nitrogen, and all solvents were freshly distilled under nitrogen prior to use. All other reagents were reagent grade quality obtained from commercial supplies and used without further purification. Thin-layer chromatography was performed on aluminium sheets coated with silica gel 60F (Merck 5554). Column chromatography was carried out by using silica gel (ICN 4663, 63-200 mesh). ^{1}H NMR spectra were recorded at 300 MHz. ^{13}C NMR spectra were recorded at 75 MHz. Mass spectra were recorded in the ESI mode. 1,1'-(pentane-1,5-diyl)dipyridinium diiodide (Space5×2I) and 1,1'-(decane-1,10-diyl)dipyridinium diiodide (Space10×2I) were synthesized according to literature procedure.[13]

General procedure for the synthesis of Au MPCs stabilized with tetraoctylammonium bromide (TOABr):

These clusters were prepared following the Schiffrin method.[12] Briefly: a 30 mM solution of $HAuCl_4$ in water (30 mL) was added to a 25 mM solution of tetraoctylammonium bromide in toluene (80 mL). The transfer of the gold salt to the toluene phase can be clearly seen visually within a few seconds. A 0.4 M solution of freshly prepared $NaBH_4$ (25 mL) was slowly added to the stirred mixture, which caused an immediate reduction to occur. After 30 min the two phases were separated and the

toluene phase was subsequently washed with 0.1M H_2SO_4 and H_2O (three times), and then dried over anhydrous Na_2SO_4.

Synthesis of C4NP Au MPCs:

to a 20 ml of TOABr stabilised NPs solution 50 mg of calix[4]arene was added and stirred for 12h at room temperature. After this period 30 ml of ethanol was added and the solution was centrifugated at 6000 rpm. After precipitation of NPs the colourless liquid was removed and the precipitate ridissolved in 40 ml of toluene and centrifugated again at 2000 rpm in order to remove the colloidal gold. The NPs solution was collected and used without any other purification .

UV-Vis Experiments:

Optical absorption spectroscopy was performed with a fiber-coupled reflection probe through the wall of the borosilicate beaker. The light from a tungsten lamp (Ocean Optics, DH 2000) was guided through the liquid with a path length of 12 mm and sent to a fiber optics spectrometer (Ocean Optics, USB2000, 250 -800 nm).

Dynamic Light Scattering Experiments :

The hydrodynamic diameter of the particles and agglomerates in solution was measured by dynamic light scattering (DLS). DLS probes the temporal autocorrelation time of the light scattered from the particles, which is directly related to their size and the properties of the solvent (refractive index and viscosity).

The measurement was taken with a home build correlator setup with a 1.2 mW HeNe laser as light source, a scattering geometry at 90 degrees in 2Θ and s polarisation. The detector was a single mode fiber coupled avalanche Geiger module (SensL) with a time resolution of 60 ns. The single photon signal was correlated with a 480ns resolution correlator (correlator.com) and read by a PC. Due to the high particle density the contrast in the autocorrelation function was limited to about 0.15, which still allowed to determine the correlation time with good precision within 2-5 minutes. The nanoparticle suspension was placed in a standard 4 sided cuvette with 10 mm path length.